

Implementation of CVR in Distribution Networks by Optimal Coordination of BESS and PV Inverters Using Arithmetic Optimization Algorithm

Mojtaba Ahanch, Roy McCann
NSF I/UCRC on GRid-connected Advanced Power Electronic Systems (GRAPES)
University of Arkansas, Fayetteville, AR 72701, U.S.A.
mahanch@uark.edu, rmccann@uark.edu

Abstract—This article proposes a new framework for the substation demand reduction and power loss minimization in distribution networks by implementing conservation voltage reduction (CVR) strategy. The proposed framework coordinates Battery Energy Storage Systems (BESS), Smart PV inverters and voltage control devices -including OLTC and voltage regulators- so that the substation demand and network power loss are reduced while the service voltage range meets the IEEE 1547 standard (120-114 V). The suggested CVR strategy is applied to the IEEE 34-bus case study system consisting of two PV generations and BESS. The smart PV inverters are controlled based on the combined Volt/VAr-Volt/Watt (VVW) characteristics scheme. Also, BESS is charged and discharged with regard to the time and peak shave control modes, respectively. The Arithmetic Optimization Algorithm (AOA) is implemented in MATLAB scripts for solving the optimization problem. Power flow studies are carried out using OpenDSS software. Results reveal that the new framework can achieve higher substation demand reduction considering the concurrent control of PVs and BESS.

Keywords—CVR, Battery Energy Storage Systems, Smart PV Inverter, Arithmetic Optimization Algorithm, OpenDSS.

I. INTRODUCTION

Solar PV generations are being commercialized worldwide due to their long-term profits, environmentally friendly nature, and very low maintenance costs. However, intermittent nature of PV systems can affect the normal operation of distribution networks [1-2]. Nonlinear characteristics of PV array are highly dependent on two volatile factors, including temperature and irradiance. Different natural and unnatural factors such as irradiation angles, passing clouds, dusts, and neighboring shadows can cause PV arrays face different irradiation level. Besides, PV arrays normally generate power around midday when the consumers' demand is much less than peak hours. One popular solution to cope with the PV system challenges is to utilize energy storages like batteries in distribution networks. Batteries can be effective in a short-term period (e.g., when the PV output drops abruptly), or in long-term when it can transfer PV power from light load periods to peak hours.¹

Conservation voltage reduction (CVR) is a conventional approach utilized by electrical utilities to save energy and cut down their load during peak hours. It decreases the service

voltage such a way that ANSI Standard C84.1 is fulfilled across the distribution systems (keeping voltages at each node between 0.95-1.05 p.u.) [3]. CVR is achieved by controlling legacy voltage control devices such as OLTCs, voltage regulators and capacitor banks within the substation or feeder, or by the new mechanisms like Volt/VAr and Volt/Watt control of renewable resources such as PV, wind turbines and storages. Several researches implemented by the utilities have shown that a 1% service voltage reduction leads to 0.3%–1% load reduction which can save billions of dollars for the utilities [4]. Besides, it has been proved that the high penetrations of various DERs in distribution networks can further enhance the CVR savings [5-6].

The revised IEEE 1547 standard requires that DERs must provide VAR compensation when requested by distribution network operators [7]. Thus, PV systems and batteries are equipped with smart inverters which allow them to inject or absorb reactive power. Hence, DERs have the ability to control the voltage locally or centralized and function as a volt/VAR control (VVC) device. Recently, researchers have introduced a variety of techniques for the efficient coordination of legacy voltage control devices and smart PV inverters [8]. In [9], the proposed methodology simultaneously coordinates traditional VVC devices and PV inverters for voltage regulation and energy saving. In [10], the authors used a new nondominated sorting genetic algorithm to solve the volt/VAR optimization (VVO). Multistage VVC operations were also introduced to effectively use traditional and advanced VVC devices, including CBs, OLTC, and PV inverter [11-13]. In [14], the researchers presented a bi-level VVO method which coordinates the legacy voltage control devices and smart inverters. It is proved that the CVR operation can be improved considerably by the reactive power dispatched from inverter-based distributed generators (IDGs) and soft open points (SOPs) [15].

Battery Energy Storage Systems (BESS) have been largely implemented in power systems aiming at power loss reduction, power quality and voltage improvement, load shaving and DER power smoothing [16]. In [17], the researchers suggested a new approach for the BESS optimal placement to minimize the total investment while implementing CVR. The proposed CVR framework in this paper coordinates BESS, PV inverters and voltage regulators using Arithmetic Optimization Algorithm (AOA) which is explained in section II. The AOA will be introduced in section III, and the results are stated in section IV.

¹This project is supported by National Science Foundation's Fundamental Research Project NSF-FRP grant no. 1747757 as part of the NSF I/UCRC program that funds the GRAPES center.

II. THE PROPOSED MODEL

A. CVR problem

In this study, the proposed model intends to decrease the substation demand and save energy while minimizing voltage deviations. The following objective function describes the CVR problem.

$$\text{Minimize} (SS_{\text{Energy}} + VD). \quad (1)$$

The substation active power demand (SS_{Energy}) consists of distribution network kW_{Load} and kW_{Loss} as are given by the following equations:

$$SS_{\text{Energy}} = \sum_{\text{time}=1}^t \sum_{i=1}^n kW_{\text{Ssdemand}}^t = \sum_{\text{time}=1}^t \sum_{i=1}^n kW_{\text{Load}}^t + kW_{\text{Loss}}^t \quad (2)$$

$$kW_{\text{Load}}^t = \sum_{\varphi=a,b,c} \sum_{m=1}^{nl} (P_{Lm}(V_m))^t \quad (3)$$

$$kW_{\text{Loss}}^t = \sum (P_{\text{Line-loss}}^t + P_{\text{Transformer-loss}}^t + P_{\text{Inv-loss}}^t) \quad (4)$$

$$P_{\text{Line-loss}} = \sum_{i=1}^N \sum_{j=1, j \neq i}^N R_{ij} * I_{ij}^2 \quad (5)$$

$$I_{ij} = (|V_i| \angle \delta_i - |V_j| \angle \delta_j) * |Y_{ij}| \angle \theta_{ij}, \quad (6)$$

where kW_{Ssdemand} , substation power demand; kW_{Loss} , active power loss of the system; kW_{Load} , active load; P_{Lm} and V_m active load and voltage; φ , phase; $P_{\text{Line-Loss}}$, line loss of the network; $P_{\text{Transformer-loss}}$, transformer total loss; and $P_{\text{Inv-loss}}$, PV inverter power.

Subject to:

$$P_i = P_{Gi} - P_{Li} = \sum_{j=1}^N |V_i V_j Y_{ij}| \cos(\theta_{ij} + \delta_j - \delta_i) \quad (7)$$

$$Q_i = Q_{Gi} - Q_{Li} = \sum_{j=1}^N |V_i V_j Y_{ij}| \sin(\theta_{ij} + \delta_j - \delta_i) \quad (8)$$

$$V_i^{\text{Min}} \leq V_i \leq V_i^{\text{Max}} \quad (9)$$

$$V_i^{\text{Min}} = 0.95 \text{ pu}, V_i^{\text{Max}} = 1.05 \text{ pu}$$

$$P_{Gi}^{\text{Min}} \leq P_{Gi} \leq P_{Gi}^{\text{Max}} \quad (10)$$

$$Q_{Gi}^{\text{Min}} \leq Q_{Gi} \leq Q_{Gi}^{\text{Max}}, \quad (11)$$

where P_{Gi} and Q_{Gi} denote the generated active and reactive power, P_{Li} and Q_{Li} represent the active and reactive load, V_i is the node voltage, P_{PVi} and Q_{PVi} are the PV active and reactive power, and PF_i is the network power factor.

VD refers to voltage deviation on the distribution network that should be minimized. VD is defined as follows [18]:

$$VD = \frac{1}{nb} \sum_{i \in nb} (1 - \mu_i) \quad (12)$$

$$\mu_i = \begin{cases} \frac{V_i - V_{\text{min}}}{V_n - V_{\text{min}}} & \text{if } V_{\text{min}} \leq V_i \leq V_n \\ \frac{V_{\text{max}} - V_i}{V_{\text{max}} - V_n} & \text{if } V_n \leq V_i \leq V_{\text{max}}, \end{cases} \quad (13)$$

where, V_n is the nominal voltage, and V_i is the voltage of the i th bus. For each bus, closer values of μ_i to 1 results in smaller voltage deviation.

B. OLTC and VRs modeling

The generalized regulation ratio of Voltage regulators and OLTC can be obtained from the following equations [19]:

$$b_{vr} = 1 + \text{Tap}_{vr} \times \frac{\Delta V_{\text{step}}}{100} \quad (14)$$

$$\Delta V_{\text{step}} = \left(\frac{S \text{ standard Voltage Regulation}}{\text{No of steps}} \right), \quad (15)$$

where, b_{vr} denotes the voltage regulation ratio of OLTC or VRs.

For OLTC:

$$\begin{aligned} b_{vr} &= \pm 10\%, \\ \text{Taps} &= [-16, \dots, 0, \dots, 16] \\ \Delta V_{\text{step}} &= 0.625\% \end{aligned} \quad (16)$$

For Voltage regulators:

$$\begin{aligned} b_{vr} &= \pm 5\%, \\ \text{Taps} &= [-8, \dots, 0, \dots, 8] \\ \Delta V_{\text{step}} &= 1.25\% \end{aligned} \quad (17)$$

Due to moving parts in OLTC and VRs, overuse of these mechanical devices can cause life cycle degradation and maintenance costs increase. Hence, maximum tap changing limits should be considered for daily operation of these device as follows:

$$\sum_{\text{time}=1}^t \text{TapChange}_{vr}^t \leq \text{TapChange}_{vr}^{\text{max}}. \quad (18)$$

C. Smart PV inverter control

The combined Volt/VAr-Volt/Watt (VVW) characteristics-based scheme was used in this study to determine the desired active and compensating reactive power from the smart PV inverters. The Volt/VAr curve is shown in Figure 1, and it is obtained by defining the four (P_1, P_2, P_3 , and P_4) parameters.

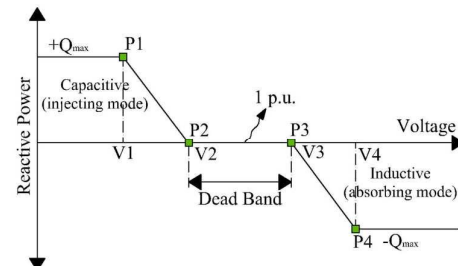


Fig. 1. Volt-VAr characteristics of smart PV inverters.

The output reactive power of Volt/VAr mode can be obtained by the following equation:

$$Q = \begin{cases} Q^{\max} & V < V_1 \\ \left(\frac{V_1 - V}{V_2 - V_1}\right) * Q^{\max} & V_1 < V < V_2 \\ 0 & V_2 < V < V_3 \\ \left(\frac{V_3 - V}{V_4 - V_3}\right) * Q^{\max} & V_3 < V < V_4 \\ -Q^{\max} & V > V_4. \end{cases} \quad (19)$$

Figure 2. illustrates the Volt-Watt curve. This mode controls the active power of PV inverter via curtailing the generated power when there is high PV generation, and the load is much lower than the PV output.

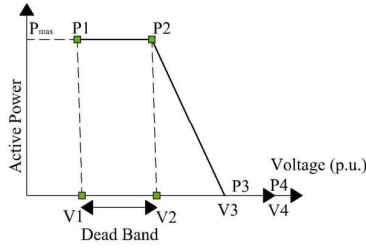


Fig. 2. Volt-Watt characteristics of smart PV inverters.

The following equation determines the total active power of PV in Volt-Watt mode:

$$P = \begin{cases} P^{\max} & V < V_2 \\ \left(\frac{V_3 - V}{V_3 - V_2}\right) * P^{\max} & V_2 < V < V_3 \\ 0 & V > V_3. \end{cases} \quad (20)$$

D. Battery Energy Storage Systems (BESS)

BESS are considered as one of the controllable distributed energy resources (DER). Advanced power electronic inverters can precisely manage the control charge and discharge systems of BESS. Thus, they can be used as a solution to the current operational and reliability problems in distribution networks. Researchers in EPRI have been modeling and evaluating the applicability of BESS in distribution network planning using OpenDSS. They have developed six modes for BESS as follows [20]:

- 1- Static mode: the BESS mode can be set manually to *discharging, charging, or idling*.
- 2- Time mode: BESS can be triggered at predefined times to discharge or charge.
- 3- Peak shave mode: BESS is triggered to discharge when the load exceeds a specified peak value.
- 4- Load following mode: The control system triggers the BESS to discharge at a specified time based on a nearly real-time load forecasting system when it is required to offset demand.
- 5- Loadshape following mode: The control system determines the charge and discharge period based on a specified form.

6- Dynamics mode: This mode is used for fast-charging models like Microgrids' frequency control

A detailed description of the modes along with examples can be found in the OpenDSS manual [21]. In this study, the peak shave mode is implemented to charge or discharge BESS.

E. Line Drop Compensation (LDC) method

OLTC/VRs tap positions are controlled using LDC method. Figure 3. represents the system consisting of the LDC operation motor, the compensation circuit and voltage relay. The circuit includes a potential transformer (PT), current transformer (CT) and impedance matching transformer.

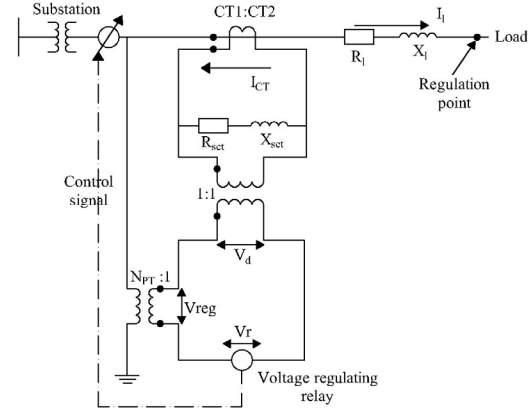


Fig. 3. Line Drop Compensation (LDC) modeling.

$R_{set\Omega}$ and $X_{set\Omega}$ denote the equivalent feeder impedance. First, the control system calculates the voltage drop between the OLTC/VRs and target load center. Considering the voltage drop coming out across the relay, it determines the voltage compensation value, and then sends control signals to the motor to changes the OLTC/VRs tap positions. The following equations describe the LDC method [19]:

$$R_{set\Omega} + X_{set\Omega} = (R_{l\Omega} + X_{l\Omega}) \cdot \frac{CT_1}{N_{PT} \cdot CT_2} \Omega \quad (21)$$

$$(R_{set\Omega} + X_{set\Omega}) \times CT_2 = R_l + jX_1 \quad (22)$$

$$R_l + jX_1 = (R_{l\Omega} + X_{l\Omega}) \times \left(\frac{CT_1}{N_{PT}} \right) V \quad (23)$$

$$V_d = (R_{set\Omega} + X_{set\Omega}) \times I_{CT} \quad (24)$$

$$V_r = V_{reg} - V_d, \quad (25)$$

where R_{set} and X_{set} represent the compensation settings, I_{CT} is the current of the compensator circuit, V_d is the voltage drop, V_{reg} denotes the input voltage of the compensator circuit, and V_r signifies the calculated voltage at the target load center needed for regulating OLTC/VRs' tap positions.

III. ARITHMETIC OPTIMIZATION ALGORITHM (AOA)

The AOA is a new metaheuristic algorithm originated from the four math operators including multiplication (M), division (D), subtraction (S), and addition (A)). Detailed descriptions of the AOA can be found in [22-23].

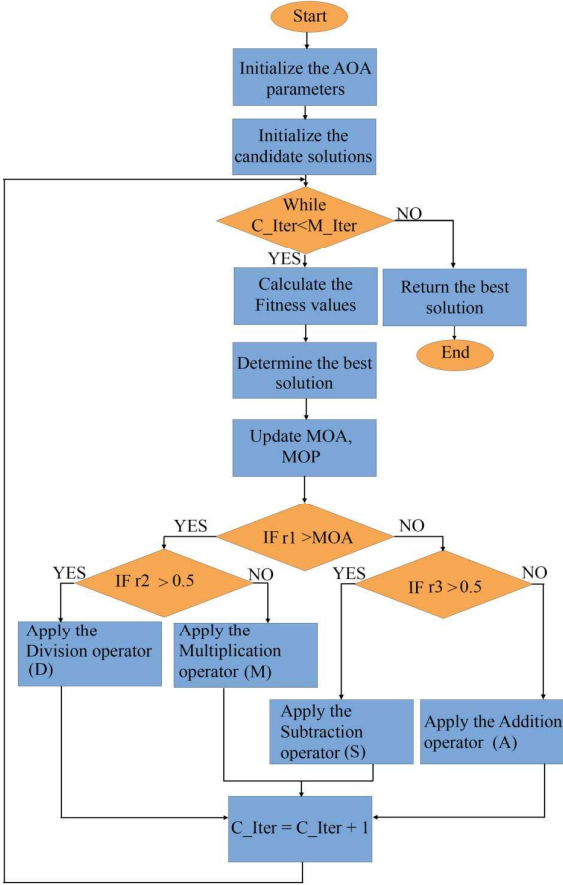


Fig. 4. AOA flowchart.

Similar to the other population-based optimization algorithms, the AOA initiates with a number of randomly generated candidate solutions. Then, the algorithm enters into the exploration and exploitation phases to find the best solutions. The AOA uses the Math Optimizer Accelerated function (MOA) to select the appropriate phase (either exploration or exploitation) for the beginning of its work. The MOA is calculated as following:

$$MOA(C_Iter) = \text{Min} + C_Iter \times \left(\frac{\text{Max} - \text{Min}}{M_Iter} \right), \quad (26)$$

Where, the *MOA* represents the value of function at the *t* iteration, *C Iter* illustrates the current iteration ($C_Iter \in [1, \dots, M_Iter]$). The *Max* and *Min* terms denote maximum and minimum values of the *MOA* function, respectively.

A. Initialization

The following equations represent the AOA' exploration model. The AOA exploration phase randomly explores the search space in order to find better solutions by employing D and M search strategies conditioned by $r2 > MOA$.

$$x_{i,j}(C_Iter+1) = \begin{cases} \text{best}(x_j) \div MOP \times ((UB_i - LB_j) \times \mu + LB_j), & r_2 < 0.5 \\ \text{best}(x_j) \times MOP \times ((UB_i - LB_j) \times \mu + LB_j), & \text{otherwise.} \end{cases} \quad (27)$$

In the above equation, $x_i(C_Iter)$ and $x_i(C_Iter+1)$ represent the current and next solutions, respectively. $\text{best}(x_i)$ denotes the *j*th location in the best solution. Also, μ , as a control parameter, adjusts the exploration search.

$$MOP(C_Iter) = 1 - \frac{C_Iter^{\alpha}}{M_Iter^{\alpha}}, \quad (28)$$

where, $MOP(C_Iter)$ is the coefficient parameter at the *t*th iteration. Besides, α represents a control parameter which is used for tuning the exploration search.

B. Initialization

The exploitation searching phase utilizes subtraction (S) and addition (A) search strategies conditioned by the value of MOA function. The following equation illustrates the S and A states.

$$x_{i,j}(C_Iter+1) = \begin{cases} \text{best}(x_j) - MOP \times ((UB_i - LB_j) \times \mu + LB_j), & r_3 < 0.5 \\ \text{best}(x_j) \times MOP \times ((UB_i - LB_j) \times \mu + LB_j), & \text{otherwise.} \end{cases} \quad (29)$$

Figure 4. shows the detailed process of AOA.

IV. SIMULATIONS AND VALIDATION

A. The proposed CVR framework

The suggested CVR framework -considering smart VVW control of solar PV inverters and the peak shave mode of BESS- was implemented on a modified IEEE 34-bus distribution test feeder. The proposed control and optimization strategies were developed in a MATLAB-COM-OpenDSS platform shown in Figure 5. As can be seen, the test system is modeled and power flow analysis is accomplished in OpenDSS, and AOA and GridPV toolbox are implemented in MATLAB. The COM interface transfers power flow results (including the line currents, nodes' voltages, and PV outputs) from OpenDSS to MATLAB and sends control signals (including OLTC/VRs' tap positions) from MATLAB to OpenDSS. The modified test system is shown in Figure 6. It consists of a 2500-kVA substation transformer with an OLTC. It has 32 tap steps which allows each tap to increase or decrease the transformer voltage by 0.3125%. Also, there are two VRs in the middle of the feeder taking care of voltage regulation throughout the network. Each of these VR has 16 tap steps so that each tap can increase or decrease their output voltage by 0.626%. A 200-kW BESS with peak shave discharge mode is considered at node 22. The hourly rated power is 800 kWh, nominal voltage is 4.16 kV, and the stored and reserve values are both 30%. Besides, two 150-kW PV generations are considered at nodes 9 and 23. The desired active and the compensating reactive power of both smart PV inverters are determined based on the combined Volt/VAr-Volt/Watt (VVW) characteristic scheme described in section II. The real time data acquisition intervals for the PV output were set at every 5 minutes. The feeder and load data are derived from [23].

B. Results and discussions

The performance of the suggested framework has been evaluated using three different scenarios considering the

VWV scheme of smart PV inverters and BESS peakshave mode as follows:

- 1- Scenario 1: Base operation; without CVR strategy
- 2- Scenario 2: With CVR strategy and without BESS
- 3- Scenario 3: With CVR strategy and BESS

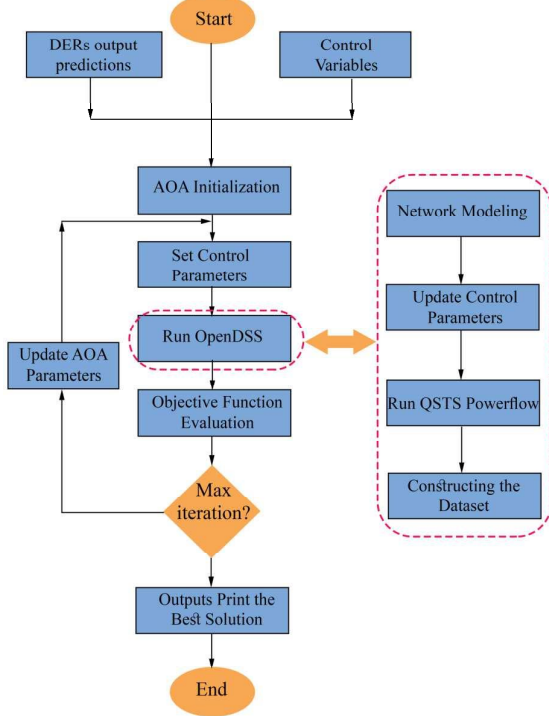


Fig. 5. The proposed method using the MATLAB-COM-OpenDSS model.

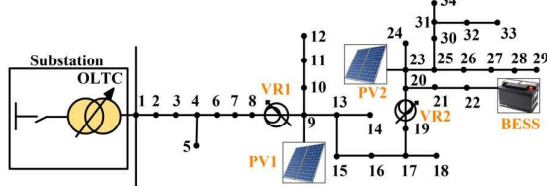


Fig. 6. Modified 34-bus residential case study system.

In this study, V_{reg} is set to 120V for OLTC and VRs assuming that the remote control is not available for voltage control devices. Besides, time delays for the OLTC and VRs are set to 30 second and 1 minutes, respectively. Maximum tap change is set 1 for each device in each step. Table 1. represents the energy received from the network and system power losses for 3 proposed scenarios.

For the first scenario 1 (without CVR and BESS), 21304 kWh is imported from the substation, and the power loss is 1951 kWh. These values are reduced to 20485 and 1867 in the second scenario (with CVR and without BESS). However, by implementing the CVR strategy and considering BESS, the energy received from substation and power loss reduce to 19889 and 1832, respectively. As can be seen, concurrent implementation of CVR and BESS can result in 6.64% and 7% reductions in power demand and power losses.

TABLE I. ENERGY AND POWER LOSS IN DIFFERENT SCENARIOS

	Energy received (kWh)	Power Loss (kWh)
Scenario 1	21304	1951
Scenario 2	20485	1867
Scenario 3	19889	1832

The following figures illustrate the results of scenario 3 over the 24-hour day ahead planning. Figure 7. shows the BESS charge and discharge planning. BESS starts charging at 3:00 am when the load is low, and discharge at around 5:00 pm which the peak load begins. Charge and discharge states are also shown in Figure 8.



Fig. 7. The BESS charge and discharge planning.

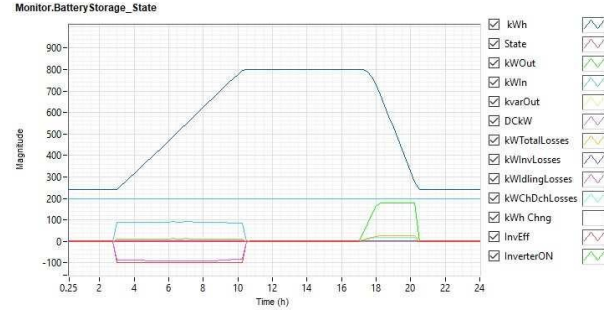


Fig. 8. The BESS charge and discharge states.

Figure 9. depicts the active and reactive power received from the substation during the day-ahead planning horizon. The imported energy is reduced around midday as the PV output is at its highest level. OLTC and VRs tap positions are also shown in Figure 10.

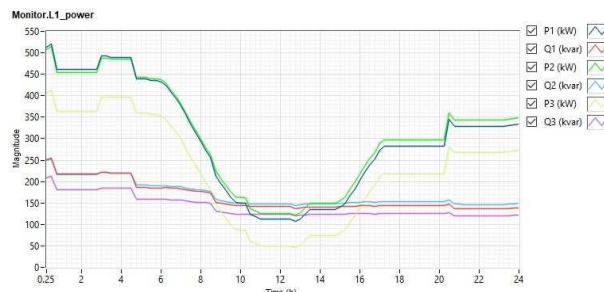


Fig. 9. Active and reactive power received from the substation.

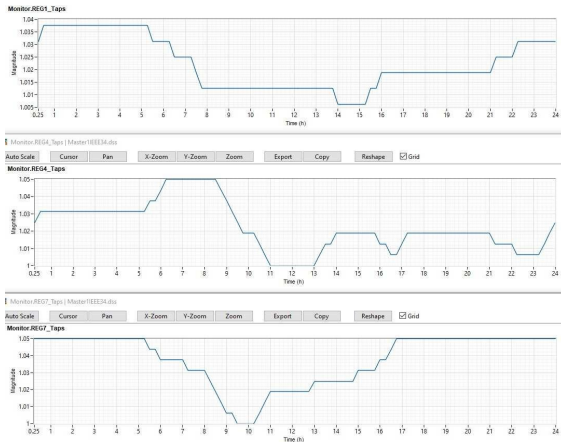


Fig. 10. Optimal OLTC and VRs' tap positions.

CONCLUSION

This paper proposed a new CVR framework for the demand and power loss minimization by optimal coordination of BESS, PV inverters, OLTC and VRs. A combined Volt/VAr-Volt/Watt scheme was introduced for controlling the PV inverters. The BESS charge and discharge states were also controlled based on the time and the peak shave modes. The impacts of the proposed framework have been seen on the IEEE 34-bus case study system with and without BESS. Findings of the simulations reveal that a considerable demand reduction can be achieved by concurrent control of smart PV inverters and BESS.

ACKNOWLEDGEMENT

Special thanks go to the National Science Foundation for the NSF-FRP grant no. 1747757. This project was carried out as part of the NSF Center on GRid-connected Advanced Power Electronic Systems (GRAPES).

REFERENCES

- [1] S. Arora, R. Khanna, S. Kaur and S. Satsangi, "Substation Energy Analysis by Combined Approach of CVR in a Distribution Network with Smart PV System," *2020 IEEE First International Conference on Smart Technologies for Power, Energy and Control (STPEC)*, 2020, pp. 1-5, doi: 10.1109/STPEC49749.2020.9297766.
- [2] D. P. Simatupang and J. Choi, "Integrated Photovoltaic Inverters Based on Unified Power Quality Conditioner with Voltage Compensation for Submarine Distribution System," *Energy*, vol. 11, no. 11, p. 2927, Oct. 2018.
- [3] S. Singh, S. Veda, S. P. Singh, R. Jain and M. M. Baggu, "Event-Driven Predictive Approach for Real-Time Volt/VAR control with CVR in solar PV rich Active Distribution Network," in *IEEE Transactions on Power Systems*, doi: 10.1109/TPWRS.2021.3057656.
- [4] Zhaoyu Wang; Jianhui Wang, "Review on implementation and assessment of conservation voltage reduction," *IEEE Trans. Power Syst.*, vol.29, no.3, pp.1306-1315, May 2014.
- [5] T V Dao, S Chaitusaney and H T N Nguyen, "Linear least-squares method for conservation voltage reduction in distribution systems with photovoltaic inverters." *IEEE Trans on Smart Grid*, vol. 8, no. 3, pp.1252-1263, 2017.
- [6] F. Ding and M. Baggu, "Coordinated Use of Smart Inverters with Legacy Voltage Regulating Devices in Distribution Systems with High Distributed PV Penetration — Increase CVR Energy Savings," *IEEE Trans on Smart Grid*. (Early access) 2018.
- [7] IEEE Standard for Interconnection and Interoperability of Distributed Energy Resources with Associated Electric Power Systems Interfaces," in IEEE Std 1547-2018 (Revision of IEEE Std 1547-2003), vol., no., pp.1-138, 6 April 2018.
- [8] V. B. Pamshetti and S. P. Singh, "Multi-Stage Coordination Volt/VAR Control with CVR in Active Distribution Network in presence of Inverter-Based DG Units and Soft Open Points," *2020 IEEE Industry Applications Society Annual Meeting*, 2020, pp. 1-8, doi: 10.1109/IAS44978.2020.9334741.
- [9] V. B. Pamshetti and S. P. Singh, "Optimal coordination of PV smart inverter and traditional volt-VAR control devices for energy cost savings and voltage regulation," *Int. Trans. Elect. Energy Syst.*, vol. 29, no. 7, 2019, Art. no. e12042.
- [10] T. S. Vitor and J. C. M. Vieira, "Operation planning and decision-making approaches for volt/VAR multi-objective optimization in power distribution systems," *Electr. Power Syst. Res.*, vol. 191, 2021, Art. no. 106874.
- [11] Y. Wang, T. Zhao, C. Ju, Y. Xu, and P. Wang, "Two-level distributed voltage/ VAR control using aggregated PV inverters in distribution networks," *IEEE Trans. Power Del.*, vol. 35, no. 4, pp. 1844–1855, Aug. 2020.
- [12] Y. Xu, Z. Y. Dong, R. Zhang, and D. J. Hill, "Multi-timescale coordinated voltage/VAR control of high renewable-penetrated distribution systems," *IEEE Trans. Power Syst.*, vol. 32, no. 6, pp. 4398–4408, Nov. 2017.
- [13] C. Zhang, Y. Xu, Z. Dong, and J. Ravishankar, "Three-stage robust inverter-based voltage/VAR control for distribution networks with high-level PV," *IEEE Trans. Smart Grid*, vol. 10, no. 1, pp. 782–793, Jan. 2019.
- [14] R. R. Jha, A. Dubey, C.-C. Liu, and K. P. Schneider, "Bi-level volt-VAR optimization to coordinate smart inverters with voltage control devices," *IEEE Trans. Power Syst.*, vol. 34, no. 3, pp. 1801–1813, May 2019.
- [15] D. Choeum and D.-H. Choi, "Vulnerability assessment of conservation voltage reduction to load redistribution attack in unbalanced active distribution networks," *IEEE Trans. Ind. Inform.*, vol. 17, no. 1, pp. 473–483, Jan. 2021.
- [16] R. K. Varma, K. B. Nanavati and S. Mohan, "Simultaneous Line Loss Minimization and CVR with Smart Inverter Control of BESS and PV System as STATCOM," *2020 IEEE Power & Energy Society General Meeting (PESGM)*, 2020, pp. 1-5, doi: 10.1109/PESGM41954.2020.9281695.
- [17] Y. Zhang, S. Ren, Z. Y. Dong, Y. Xu, K. Meng, and Y. Zheng, "Optimal placement of battery energy storage in distribution networks considering conservation voltage reduction and stochastic load composition," *IET Gener. Transm. Distrib.*, vol. 11, no. 15, pp. 3862–3870, 2017.
- [18] D. A. Quijano and A. P. Feltrin, "Assessment of Conservation Voltage Reduction effects in networks with distributed generators," *2015 IEEE PES Innovative Smart Grid Technologies Latin America (ISGT LATAM)*, Montevideo, Uruguay, 2015, pp. 393-398, doi: 10.1109/ISGT-LA.2015.7381188.
- [19] S. Arora, S. Satsangi, S. Kaur, and R. Khanna, "Substation demand reduction by CVR enabled intelligent PV inverter control functions in distribution systems," *Int Trans Electr Energ Syst*, vol. 31, no. 2, Dec. 2020, doi: 10.1002/2050-7038.12724.
- [20] R. C. Dugan, J. A. Taylor and D. Montenegro, "Energy Storage Modeling for Distribution Planning," in *IEEE Transactions on Industry Applications*, vol. 53, no. 2, pp. 954-962, March-April 2017, doi: 10.1109/TIA.2016.2639455.
- [21] OpenDSS Program [Online], Available: <https://sourceforge.net/projects/electricdss/>
- [22] L. Abualigah, A. Diabat, S. Mirjalili, M. Abd Elaziz, and A. H. Gandomi, "The Arithmetic Optimization Algorithm," *Computer Methods in Applied Mechanics and Engineering*, vol. 376, p. 113609, Apr. 2021, doi: 10.1016/j.cma.2020.113609.
- [23] M. Ahanch and R. McCann, "Integrated Volt/Var Control and Conservation Voltage Reduction in Unbalanced Distribution Networks Considering Smart PV Inverter Control Using Equilibrium Optimizer Algorithm," *2021 IEEE Kansas Power and Energy Conference (KPEC)*, 2021, pp. 1-6, doi: 10.1109/KPEC51835.2021.9446226.